

CORRELATED DYNAMICS OF HOT AND COOL PLASMAS IN TWO SOLAR FLARES

B. Kliem¹, I. E. Dammasch², W. Curdt², and K. Wilhelm²

¹*Astrophysikalisches Institut Potsdam, An der Sternwarte 16, 14482 Potsdam, Germany*

²*Max-Planck-Institut für Aeronomie, 37191 Katlenburg-Lindau, Germany*

ABSTRACT

In flare-watch observations using the SUMER spectrometer on board *SOHO*, two limb flares were found to show correlated brightenings and line shifts of hot ($T_e \sim 10^7$ K) and cool ($T_e \sim 10^4$ K) plasmas. The brightenings occurred essentially simultaneously but the cool plasma emission decayed much earlier than the hot plasma emission, which excludes an origin in passive cooling of postflare loops and points to an active role for the cool plasma in the flare dynamics. The observations are consistent with magnetic reconnection that is triggered and sustained by the formation of a coronal condensation through the thermal instability. An MHD simulation supporting this model is presented.

INTRODUCTION

Flares are usually regarded to be “hot phenomena”: coronal and chromospheric plasma is heated to $\sim (10\text{--}30)$ MK and particles are accelerated to $\sim (10\text{--}100)$ keV or higher (e.g., Sturrock, 1980; Hudson, 1994; Kosugi, 1994). The energy stored in the magnetic field is converted suddenly and locally into kinetic energy of the plasma. Cooling plasma is observed *after* the impulsive energy release of many flares in X rays, the UV, and down to temperatures visible in $H\alpha$. However, the idea that cooling plasma at temperatures of a few 10^4 K may play a role in *initiating* flares is not commonly included in flare models. It was considered as a possibility to accelerate the tearing mode in the corona by Van Hoven *et al.* (1984), but appears to have not been pursued further since then.

Recently we have obtained spectroscopic observations of a solar limb flare using a number of emission lines in the far-UV range. A strong correlation between the initial brightenings, the line shifts, and the excess line widths of hot ($\sim 10^7$ K) and cool ($\sim 10^4$ K) plasmas was found. There were no indications of a prominence near the flare site. The correlations in the spectra and the early decay of the cool plasma brightness indicated an active role of cool plasma in the main (and probably also in the impulsive) phase of this flare, different from the usual picture of emergence through (passive) cooling of evaporated chromospheric plasma after the impulsive phase. We have suggested a model in which localized cooling of coronal plasma by the thermal instability triggers magnetic reconnection through the resulting enhanced resistivity, the combined processes leading to the correlated dynamics of hot and cool plasmas in a loop-loop interaction geometry (Damasch *et al.*, 2001; Kliem *et al.*, 2002). *Yohkoh/SXT* and *SOHO/EIT* data have been essential in guiding the interpretation by

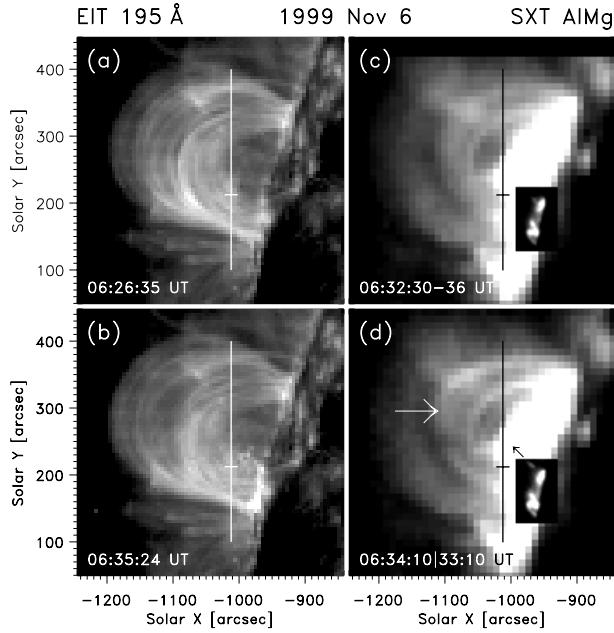


Fig. 1. Morphology of the flare in which the correlated behavior of the hot and cool plasma was discovered. (a, b) *SOHO*/EIT images just before the event and at the time of peak soft X-ray (SXR) emission; (c, d) composites of quarter-resolution and full-resolution *Yohkoh*/*SXT* images. The fixed position of the SUMER slit and the position of the cool plasma brightening at the slit are indicated. The effects seen by SUMER appeared to be associated with the weak loop-shaped brightening inside the arcade of post-flare loops of a previous flare and with the weaker (the northern) of the two *SXT* footpoint sources, which gave rise to a weak ejection that faded before the SXR emission peaked (indicated by the small arrow). The lack of any brightening in the SUMER Fe XII observations (Fig. 2) indicates that this brightening actually occurred in the Ca XVII or Fe XXIV lines which fall in the EIT passband at 195 Å. The strong EIT footpoint brightening, the southern *SXT* source, and the ascending *SXT* loop (marked by the large arrow) were associated with a separately flaring substructure in the same event. See Kliem *et al.* (2002) for further details.

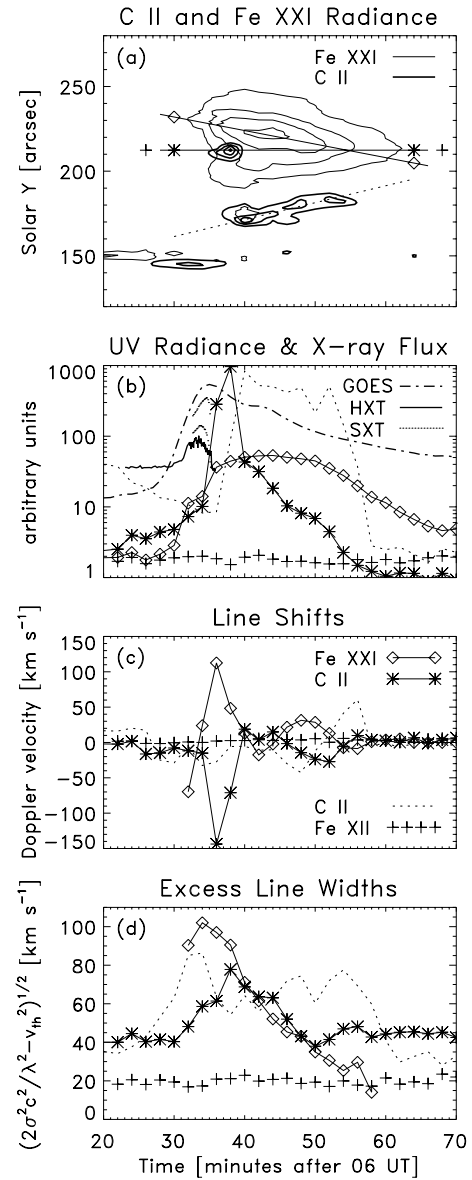


Fig. 2. Summary of SUMER data of the 1999 Nov 6 flare. (a) Equidistant isocontours of line-integrated radiance (linear scale, 20%–92% of max.) showing the flare-related brightenings in Fe XXI $\lambda 1354.1$ ($T_e \approx 10^7$ K; *light contours*) and C II $\lambda 1335.7$ ($T_e \approx 2 \times 10^4$ K; *heavy contours*). Cut lines, along which the time profiles are plotted in (b)–(d), are indicated. (b) Time profiles of line-integrated UV radiance, of the *GOES* 0.5–4 Å flux, of the *Yohkoh*/*HXT* 14–23 keV flux, and of the two footpoint sources resolved by *Yohkoh*/*SXT*. SUMER data points are plotted at the center of each 2 minutes exposure interval. (c) Line shifts relative to the average pre-flare line positions. (d) Excess line widths, where σ is the standard deviation of a Gaussian fit and v_{th} is the thermal velocity of the ion.

showing that the correlated dynamics did not arise in the loop arcade of a preceding flare but did occur inside this arcade close to the position where a new, presumably very hot loop was formed and that the event as a whole was not eruptive (Fig. 1). The *Yohkoh*/HXT provided the timing of the impulsive flare phase with respect to the UV data. UV data of this flare are shown in Figure 2, along with the X-ray time profiles.

NEW OBSERVATIONS

Data of a second event that showed a correlated brightening and line shift signature of hot (Fe XIX $\lambda 1118.1$; $T_e \approx 8$ MK) and cool (S III $\lambda 1113.2$; $T_e \approx 30\,000$ K) plasmas are displayed in Figure 3. The peak brightenings in this flare coincided exactly (at a spatial resolution along the slit of $1''$ and a temporal resolution of 170 s). As in the event on 1999 Nov 6, the brightening of the cool plasma decayed much earlier than the brightening of the hot plasma. The line shifts showed a simultaneous rise, to the red for both lines, at the onset of the brightenings, the subsequent evolution being different in detail. The main spectral properties suggest a physical relationship between the hot and cool plasmas also for this flare. Again, the cool plasma could not emerge from cooling postflare loops. A series of EIT 195 Å images that includes the time of the flare contains a weak indication that diffuse absorbing (i.e., cool) material was permanently present, extending from the disk out to about the position where the event seen by SUMER occurred. Activity in this cool material that caused a brightening of the S III line – presumably a condensation – appears to have triggered the energy release that led to the Fe XIX brightening. No *Yohkoh* or *TRACE* observations are available for this event.

This flare occurred in the decay phase of a long-duration flare at a remote location and did not produce a signature in the *GOES* light curve, which limits its magnitude to *GOES* class C3. Both cases observed so far are rather small flares. Further observations are required to see whether this is a systematic property.

FIRST SIMULATIONS OF CONDENSATION-DRIVEN MAGNETIC RECONNECTION

To test the hypothesis that a coronal condensation can trigger magnetic reconnection, we have performed two-dimensional MHD simulations of the evolution of a temperature perturbation in a coronal current sheet. The standard resistive and compressional MHD equations were integrated in a numerical setup similar to that used by Kliem *et al.* (2000) but with radiative losses included. The classical Spitzer resistivity was chosen. Its strong temperature dependence, $\eta \propto T^{-3/2}$, is the basis of our hypothesis, since it implies an increase of the resistivity by three orders of magnitude if the temperature drops from coronal to upper chromospheric values. A one-dimensional isothermal Harris current sheet equilibrium, $\mathbf{B} = B_0 \tanh(y/l_0)\mathbf{e}_x$, balanced by a density gradient across the sheet, was initially perturbed by an isobaric temperature drop in the center of the sheet, extending along the sheet by about one sheet width ($2l_0$). The parameters external to the sheet were chosen to be $T_0 = 2$ MK, Alfvén velocity $V_{A0} = 800$ km s $^{-1}$, Lundquist number $S = 2000$, plasma beta $\beta = 0.1$, and density $n_0 = 5.6 \times 10^{16} (l_0/\text{cm})^{-1}$ cm $^{-3}$.

The initial temperature perturbation developed into a condensation with the temperature decreasing to $\approx 20\,000$ K, a value which is determined by the drop of the radiative loss function. The condensation process continued during the whole simulation, with cooling material streaming into the perturbed area. Magnetic reconnection gradually commenced early in the evolution, developing the typical magnetic and velocity field pattern during the first $\approx 10^2$ Alfvén times (i.e., during ≈ 1 min; $\tau_A = l_0/V_{A0} = 0.7$ s for $n_0 = 10^9$ cm $^{-3}$), and continued also during the whole simulation. The condensation-reconnection process was followed for several $10^2 \tau_A$ (Fig. 4). It turned out to be less vigorous than reconnection driven by anomalous resistivity because the reconnection outflow jets are not accelerated right from the X line but only from the outer boundary of the condensation, but outflow velocities of ≈ 50 km s $^{-1}$ – of the same order as the observed Doppler velocities – were reached. These simulations support our hypothesis that localized condensations, formed by the thermal instability, can trigger and sustain magnetic reconnection in solar flares. To obtain a more complete picture of the condensation-reconnection process, the stabilizing influence of thermal conduction has to be included, which will be the subject of future investigations.

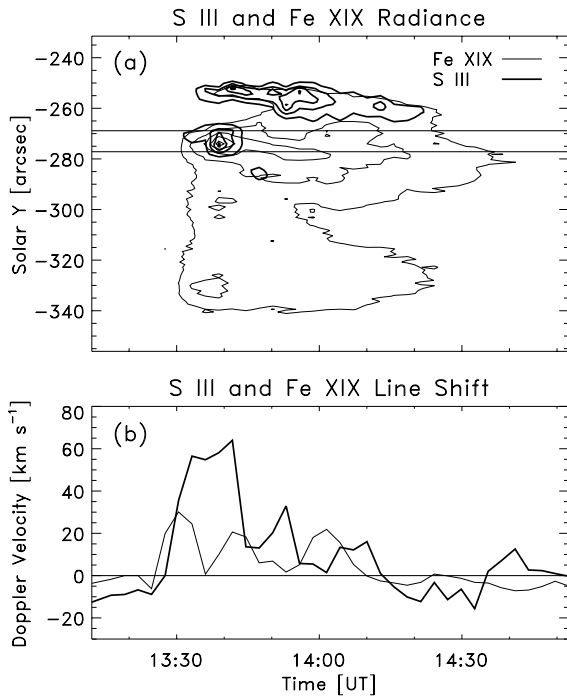


Fig. 3. SUMER data of the 2000 Oct 25 flare taken at a fixed off-limb pointing, $(x, y) = (-1000'', -300'')$, with a cadence of 170 s. (a) Equidistant isocontours of line-integrated radiance (linear scale, 15%–90% of maximum) showing the flare-related brightenings in Fe XIX $\lambda 1118.1$ (light contours) and S III $\lambda 1113.2$ (heavy contours). (b) Fe XIX and S III line shifts, averaged over the range $-277'' < y < -269''$ as indicated in (a).

ACKNOWLEDGEMENTS

We thank D. E. McKenzie and J. Sato for providing us with reduced *Yohkoh* data. The EIT, SXT, and HXT data are courtesy of the *SOHO*/EIT and the *Yohkoh*/SXT and HXT consortiums, respectively. The SUMER project is financially supported by DLR, CNES, NASA, and the ESA PRODEX programme. The work of BK was also supported by the EU under Contract No. HPRN-CT-2000-00153. The John von Neumann-Institut für Computing, Jülich, granted Cray computer time.

REFERENCES

- Dammasch, I.E., B. Kliem, W. Curdt, & K. Wilhelm, *Proc. IAU Symp.*, **203**, 264 (2001).
Hudson, H.S., in *New Look at the Sun*, Proc. Kofu Symp., ed. S. Enome & T. Hirayama, Nobeyama Radio Observatory, NRO Report 360, p. 1 (1994).
Kliem, B., M. Karlický, & A.O. Benz, *Astron. Astrophys.*, **360**, 715 (2000).
Kliem, B., I.E. Dammasch, W. Curdt, & K. Wilhelm, *Astrophys. J.*, **568**, L61 (2002).
Kosugi, T., in *New Look at the Sun*, Proc. Kofu Symp., ed. S. Enome & T. Hirayama, Nobeyama Radio Observatory, NRO Report 360, p. 11 (1994).
Sturrock, P.A. (ed.) *Solar Flares, A Monograph from the Skylab Solar Workshop II*, Colorado Associated University Press (1980).
Van Hoven, G., T. Tachi, & R.S. Steinolfson, *Astrophys. J.*, **280**, 391 (1984).

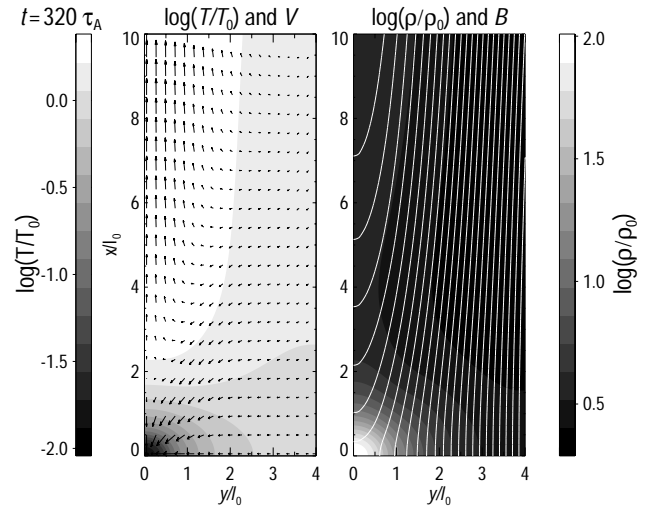


Fig. 4. Snapshot of magnetic reconnection in a two-dimensional resistive, compressible MHD simulation, induced by radiative cooling of an initial isobaric temperature drop at the origin. Displayed are temperature and velocity field (left) and density and magnetic field lines (right); $T_0 = 2 \times 10^6$ K; l_0 — initial current sheet half width; τ_A — Alfvén time (see text for further parameter values).